J Pharm Innov (2007) 2:125–134
DOI 10.1007/s12247-007-9014-y

RESEARCH ARTICLE

# Integrated Sensing and Processing Acoustic Resonance Spectrometry (ISP-ARS) for Sample Classification

**Joseph P. Medendorp · Jason A. Fackler · Craig C. Douglas · Robert A. Lodder**

Published online: 14 December 2007


**Abstract** This research introduces a novel process analytical technique, integrated sensing and processing acoustic resonance spectrometry (ISP-ARS), and compares ISP-ARS with conventional full-spectrum ARS for the characterization of solid fuel premixes used in a new pill safe designed to protect narcotics. In ISP-ARS, the acoustic excitation waveform is the analog implementation of the chemometric weight function, encoded for this work on an MP3 player and used to distinguish between fuel samples, sparing post-collection multivariate computation. In effect, the detector directly outputs the sample identity. Repeated measurements of batches of similar fuel mixtures over time produce an automatic projection of similar spectra into corresponding three-dimensional probability density contours, thus, forming the analyte classification directly. For the characterization of ten different fuel mixtures, full spectral ARS resulted in a median intermixture distance in multidimensional standard deviations (MSDs) of 185.1, while ISP-ARS resulted in a median MSD distance of 81.3. The median cross-validation MSD was 1.41 for the ARS and 1.58 for the ISP-ARS. Distances in MSDs greater than three are considered separable, and MSDs less than three are indistinguishable. The classification procedure correctly identified all samples for both analytical techniques. ISP-ARS is an effective, simpler, and more rapid alternative to full spectrum ARS that can be implemented with a commercial MP3 player and used as an inexpensive spectrometric sensor for dynamic data-driven application simulations (DDDAS) and process analytical applications.

**Keywords** PillSafe · Process analytical technology · Linear discriminant analysis · Solid fuel

J. A. Fackler · R. A. Lodder (✉)
Department of Chemistry, University of Kentucky,
A123 ASTeCC Building,
Lexington, KY 40506-0286, USA
e-mail: Lodder@uky.edu

J. P. Medendorp · R. A. Lodder
Department of Pharmaceutical Sciences, University of Kentucky,
Lexington, KY 40536, USA

C. C. Douglas
Department of Computer Science, University of Kentucky,
Lexington, KY 40506, USA

## Introduction

*Acoustic Spectrometry* Scientists know that vibrations originating from the surface of a drum, for example, contain significant acoustic clues to its shape. In a study completed in 2000, Kunkler-Peck and Turvey [1] found that individuals could distinguish whether a vibrating plate hidden from view is circular, rectangular, or triangular. The specific sound frequencies and intensities influence auditory-shape perception. In one experiment, eight volunteers assigned relatively accurate estimates to the heights and widths of three concealed, rectangular steel plates. The plates were hung behind a screen and struck by a pendulum controlled by each listener. Using the same apparatus, another eight participants discerned the dimensions of vibrating steel, wood, and Plexiglas plates. In further trials, volunteers successfully identified as circular, rectangular, or triangular each of a series of plates from these materials. These experiments demonstrate that information regarding the size, shape, and material composition of samples can be determined by human pattern recognition using only

acoustic signals. The same power is exploited in acoustic spectrometry to analyze samples with a computer.

Acoustic spectrometry is of new interest because it has potential as a means of pharmaceutical process control. Pharmaceutical industry production difficulties lead directly to higher drug prices. The US Food and Drug Administration (FDA) has noted that US drug products are of generally high quality, but there is an increasing trend toward manufacturing-related problems that lead to recalls, disruption of manufacturing operations, and loss of availability of essential drugs [2]. Low manufacturing process efficiency (<30%) has also led to increased cost of drugs. Emphasis on current good manufacturing practice (cGMP) as the means of controlling drug quality has led to reluctance among companies to innovate in the manufacturing sector. Such problems have led the FDA to conclude that a new scientific understanding of the drug production process achieved with new sensing technologies can provide science- and risk-based approaches to the regulation of drug quality, thereby, alleviating the manufacturing problems. Process analytical technologies (PAT) like near-infrared (NIR) spectroscopy and acoustic resonance (AR) have been selected as the model for the US to use in shifting successfully from empirical standards like cGMP to science-based standards for achieving manufacturing process quality.

In PAT, pattern recognition procedures are usually applied to interpret the complex output of spectrometric process sensors and to provide a reading of characteristics like active pharmaceutical ingredient (API) concentration in a drug. The false sample problem arises in pattern recognition when the pattern-recognition algorithm is presented with a sample unlike any in the original calibration set. Under such circumstances, it is possible that the algorithm will predict a reasonable API concentration even when the sample is a foreign object instead of the expected drug product. The problem is exacerbated by the chance that a foreign object might have a similar spectrum to the drug (isospectrality). The pharmaceutical industry must learn the analytical limitations of ARS for drug products, which appear to ARS as very similar to the drums of Kunkler-Peck and Turvey.

In 1966, Kac [3] put forward the question, "Can one always hear the shape of a drum?" Kac was referring to the question of whether the Laplacian operator with Dirichlet boundary conditions could ever have identical spectra on two distinct planar regions. Gordon, et al. [4] finally answered the question in the negative using an elegantly constructed counterexample [5, 6].

The simplest form of the Gordon, et al. example is a pair of regions bounded by eight-sided polygons referred to as GWW isospectral drums. Several similar examples have since been discovered [7]. The simplest and most versatile proof of isospectrality utilizes "transplantation" of the eigenfunctions [8]. The regions are composed of nonoverlapping translations, rotations, and reflections of a single shape, such as a triangle. Given an eigenfunction on one region, it is possible to prescribe a function over the other region whose values over each portion are linear combinations of the eigenfunction values over some of the portions of the first region. The combinations are selected to satisfy the boundary conditions and to correspond to values and derivatives at interfaces between portions, and the interior equation is satisfied by superposition. Therefore, the result is an eigenfunction of the second region having the same eigenvalue. To complete the proof of isospectrality, it is only necessary to confirm that the procedure is invertible. Of course, the proof is nonconstructive and other information, mainly the actual amounts of the eigenvalues, remains unknown. The net result is that if sample shape is the only factor determining whether the right pill is getting into the right bottle, one cannot always be certain of the result with only an acoustic sensor.

Numerical computation is the obvious means to find the eigenvalues to model such systems. However, straightforward numerical procedures for computing the eigenvalues are inefficient because of the existence of reentrant corners [9]. Even an adaptive approach, such as Bank's PLTMG [10], achieves very slow convergence for the eigenvalue estimates. Another well-known method for eigenvalue problems, the method of particular solutions [11], is unable to generate estimates of accuracy better than a few percent. Thus, improved methods for selecting the best algorithms are crucial, and these are being actively researched.

Shape, while a valuable characteristic, is fortunately not the only difference between finished pharmaceutical dosage forms, however. To an acoustic spectrometric sensor, pharmaceutical samples resemble Kunkler-Peck and Turvey's vibrating plates more than Kac's drum. The material composition of pharmaceutical samples varies widely, leading to differences in density and acoustic velocity that dramatically change the acoustic resonance spectra of pharmaceuticals.

*Integrated Sensing and Processing* Integrated sensing and processing acoustic resonance spectrometry (ISP-ARS) can be used as an alternative to conventional Fourier transform (FT)-ARS for the characterization of solid fuel mixes. ISP is a paradigm for the implementation of mathematics and chemometrics directly in the physical design of sensors for the purpose of data reduction [12]. Each new generation of computerized sensors and spectrometers produce more and more information obscured in data sets of higher and higher dimension. A data set from the FT-acoustic resonance spectrometer used in this research contains $n$ data points, where $n$ is the product of

sampling rate and duration. Even in low-frequency ultrasound applications, the resulting data vector contains a large number of variables (44.1 KHz×3 s=132,300 points per spectrum). After data collection, a multivariate chemometric algorithm, such as classical/partial least squares, principal component regression, or multiple analysis of variance (MANOVA) must be applied to the data set first to determine which frequencies correspond to the analyte of interest (calibration) and again to actually predict individual samples. For experiments requiring the collection of multiple spectra for multiple analytes, the computational burden of conventional FT-ARS is apparent.

Conventional AR spectrometry has previously been used for the analysis of pharmaceutical tablets [13–14], semisolids, and colloidal dispersions [15–16], liquids [17–19], and powders [20–22]. To the authors' knowledge, this research presents the first application of ISP-ARS and its comparison to full spectrum ARS. ISP-ARS is distinctive in that it does not rely exclusively on a scanning resonant waveform, as was the case with early AR spectrometry, or the signal attenuation and time delay associated with active pulse acoustics. Instead, it relies on the excitation of key frequencies identified statistically (by MANOVA in this work) specifically for the maximization of intercluster distances and the minimization of intra-cluster distances. The samples tested in this research comprise different mixtures of ammonium perchlorate ($NH_4ClO_4$), aluminum powder (Al), iron oxide ($Fe_2O_3$), casting resin, and curing agent, the combination of which make up the fuel for the PillSafe, a narcotics distribution-control product produced by RAMM, LLC [23]. Different fuel burn characteristics (e.g., time to ignition, and burn duration) result from different concentrations of the individual components in fuel premixes. There is a wide range of performance between mixes, a fact that has also been noted in the literature [23]. An analytical method capable of rapidly and accurately characterizing premixes for burning can answer important questions about performance, and optimize reaction rate for different kinds and sizes of tablets in the PillSafe.

*Controlled Substances in the PillSafe* The PillSafe is a new tamper-resistant pill bottle designed by RAMM for narcotics of abuse. The PillSafe uses fuel mixtures to destroy the tablets contained within it when necessary. In the PillSafe, drug tablets are stacked next to fuel rods. Attempts to force the dispensing mechanism to dispense off the prescribed times, or to bypass the dispensing mechanism and penetrate the bottle, cause instant destruction of the PillSafe contents. Different fuel mixtures are best for different drugs and tablet numbers. The container functions as a novel, inexpensive "Thermos"-type bottle with a microcontroller and a pressure relief system that safely destroys tablets in 2–3 s. PillSafes are designed to be registered to users at the time a prescription is filled. The PillSafe provides another line of defense to prevent theft of prescription drugs and makes illicit diversion of tablets more difficult [23].

This study focused on ISP-ARS for classifying fuel mixtures used for various content and loading configurations of the PillSafe. A detailed description of the basic AR spectrometer components has appeared elsewhere [14–15]. The new ISP-ARS used in this research encoded the excitation signal (ISP waveform) in such a way that *the detector automatically output the classification of each fuel premix as a unique voltage*. The ISP calibration began with acoustic excitation across a spectral range (0–22.05 KHz) using a broadband (white) noise source, as done with conventional FT-ARS. Using the 22-kHz spectral range, the broadband excitation signal could be loaded into an inexpensive MP3 player, producing a simple and novel process spectrometer into which multiple different calibrations could easily be downloaded over the World Wide Web. As illustrated in Fig. 1, the AR spectrometer displayed two large resonant peak structures at 10–12 and 14–17 kHz, making these useful regions to study for fuel classification purposes.

In ARS, the resonance peak frequencies and intensities shift in response to physical properties of samples such as density, viscosity, acoustic velocity and absorption, pressure, concentration, analyte size, and particle distribution. These properties are what the experimenter correlates to the observed changes in instrumental response. Whether the goal of the experiment is quantification or classification, multivariate statistics can be used to calculate a calibration-weighting function that is applied to each new spectrum. This projection of spectra into a new space of reduced dimension can be accomplished in one of two ways. The first way involves varying the excitation duration and/or intensity at particular frequencies such that each frequency is weighted according to its importance in the regression (encoding the excitation signal). The second way to accomplish the projection in analog hardware is by analog multiplication of the detected signal with an acoustic weight function after collection (post-collection) [24]. As illustrated in Fig. 2, conventional ARS consists of six steps:

(1) A white noise signal source is used to excite all frequencies with equal amplitudes simultaneously.

(2) The transmitting piezoelectric transducer (PZT) launches the signal through a quartz rod that is in mechanical contact with the fuel sample, which creates a standing wave resonant system.

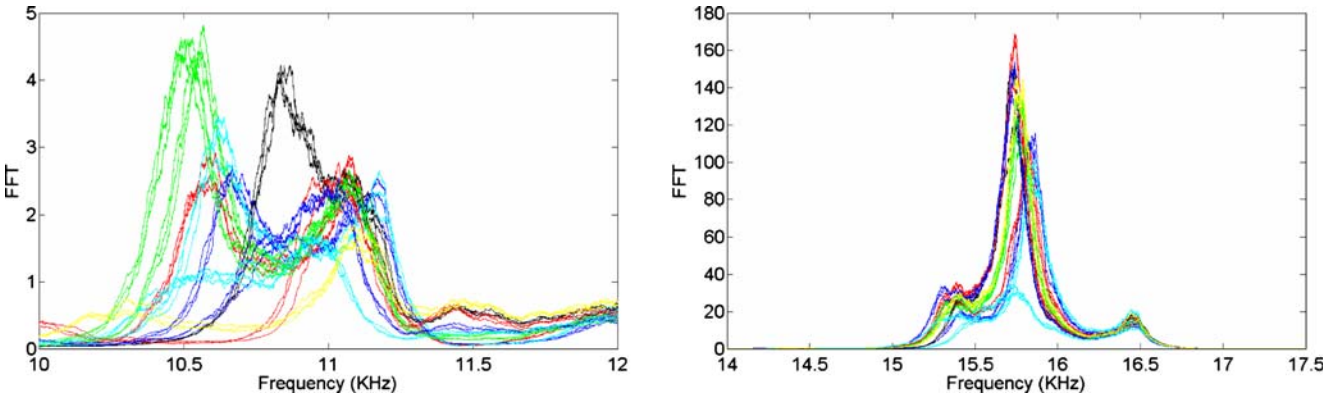


**Fig. 1** In its current configuration, the ARS has two large resonance peaks (10–12 and 14–17 kHz). The spectral features shift in frequency and in amplitude as a response to changes in physical properties of the analyte. It is this property that allows for the quantification and classification of analytes using this resonant system

(3) The resonance frequency spectrum from each calibration sample is collected with a computer sound card or an analog/digital converter.

(4) Using multivariate statistical methods (e.g., partial least squares or MANOVA), the weighting function that accentuates the relationship between the most important frequencies/spectral features and the classification or analyte concentration is calculated.

(5) This weighting function is multiplied by the frequency spectrum for all new samples using a computer that both collects the data and performs post-collection chemometric procedures, giving

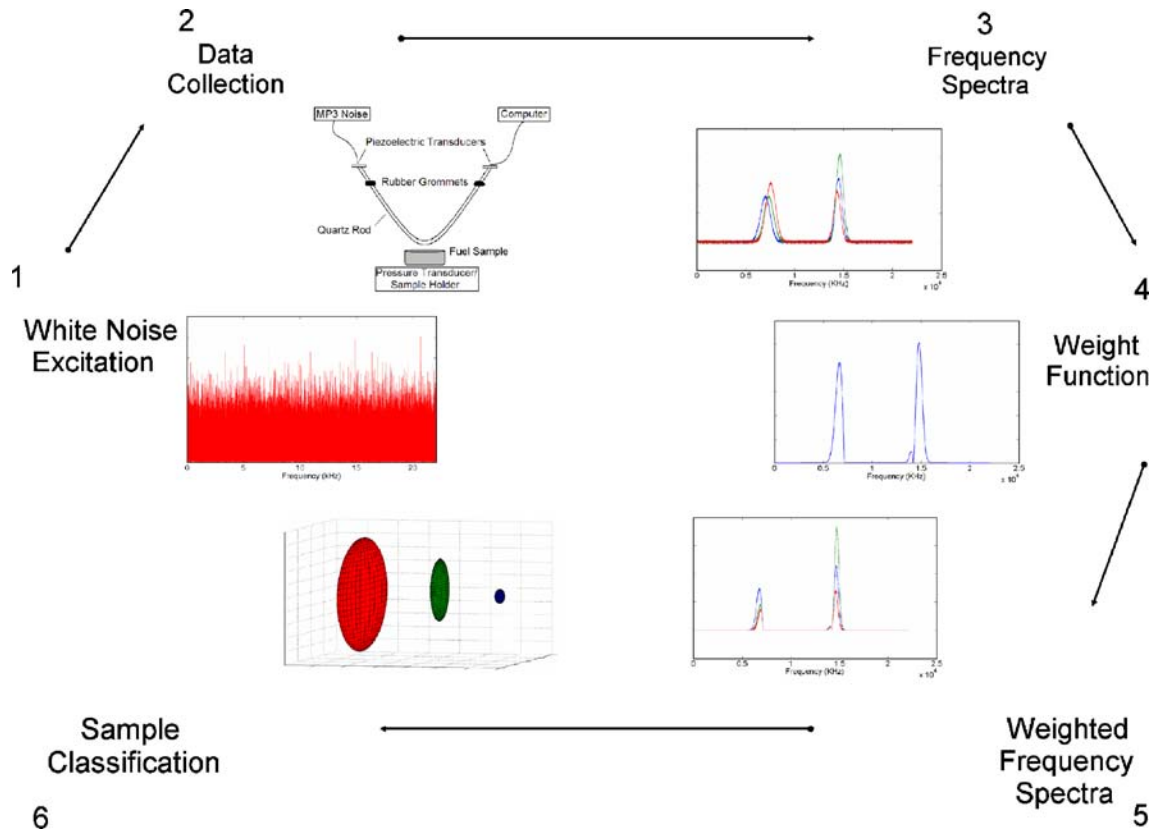


**Fig. 2** This figure illustrates conventional AR spectrometry with a broadband excitation source. When collecting full spectrum ARS, multivariate statistics are required to correlate the spectral features to the changing physical property of interest. Regression techniques, principal components, and multiple analysis of variance can be used to calculate a weight vector for use as the new ISP-ARS signal source

(6) the sample classification through discriminant analysis or analyte quantification through regression.

Alternatively, ISP-ARS effectively replaces the last two steps with:

(5) excitation with the ISP waveform calculated as in step 4 and

(6) integrated data collection and analyte classification in the sensor. In this research, the data collection step is coupled with analyte classification by projection onto a three-dimensional plot of the selected frequency combinations.

ISP-ARS offers multiplex and throughput advantages over scanning AR spectrometry similar to those offered by FT-ARS. In addition, however, ISP-ARS reduces data analysis times and the computational burden (the "*ISP advantage*") because ISP-ARS requires no post-collection Fourier transform of the data. In fact, ISP-ARS goes even further and provides instant output of analyte identity from the detector without the need for post-collection computation. In place of the white noise excitation signal, the weighting MP3 function is used as the excitation source directly. Because the system resonant frequencies are a product of the physical components of the system and the physical properties correlate to the chemical composition, the weighting function excitation produces analyte classification without the need for further computation. In this way, ISP-ARS eliminates the entire digital detection component of the ARS and enables an MP3 player alone to become a complete spectrometric sensing system.

*Theory* Analytical methods are often directed toward one of two objectives, *analyte quantification*, as in multivariate calibration, or *analyte classification*, such as undirected data mining (e.g., cluster analysis). Analyte classification is sometimes intended to reveal the underlying structure of a data set (as in this research). In addition, there are two types of data mining for analyte classification, supervised and unsupervised. In unsupervised data mining, no a priori information is given about the data structure as it relates to the classes from which the data are comprised. Conversely, supervised data mining uses prior knowledge of classes to help identify the structure. For this ISP-ARS experiment, class data are used to identify the key spectral features. MANOVA is employed to identify the frequencies that can be used to maximize between-cluster distances while minimizing same-cluster distances [25]. Once these frequencies are selected, they are encoded as the new excitation source, enabling the classification of new incoming samples without the need for further computation.

A sensing system like ISP-ARS is ideally suited for use with process simulations that can dynamically accept and respond to "online" pharmaceutical process measurements and/or can control such measurements. Conventional process simulations are conducted with static data inputs. In the new dynamic, data-driven application systems now envisioned, collected process data will be used in an "online" manner to guide the simulations. At the same time, the simulations can be used to control processes and/or the timing and targets of other process measurements. Thus, the simulations and the processes become a real-time symbiotic feedback system instead of the usual static, disjoint, and serialized approach to process simulation and control.

## Experimental Section

*Mixture Preparation* Solid fuel mixtures consisted of combinations of ammonium perchlorate ($NH_4ClO_4$), aluminum powder (Al), iron oxide ($Fe_2O_3$), casting resin (Bisphenol A/Epichlorohydrin), and polyamide curing agent (Versamid 140; Firefox Enterprises, Pocatello, ID). The percentages of each component in a sample were calculated to force them to be uncorrelated to the other components (see Table 1). The casting resin and curing agent were heated to 35°C on a hot plate. Powders were hand-blended before addition of casting and curing agents to create a homogenous mixture. The casting and curing agent were added to the powder mixtures and stirred vigorously for 3 min. Fuel mixtures were cast into plastic mini-Petri dishes of equal size to ensure equal volumes for each sample. Samples were allowed to cure for 48 h before scanning. The resulting thin mixture disks share structural similarities with Kac drums and with Kunkler-Peck and Turvey vibrating plates.

*ARS Data Collection* Samples were placed on a scale (Model 3120, Health O Meter, Bridgeview, IL, USA) to

**Table 1** Compositions of sample mixtures

| Mixture | Al | $NH_4ClO_4$ | $Fe_2O_3$ | Epoxy | Curing | Ignition | Burn |
|---|---|---|---|---|---|---|---|
| 1 | 17.07 | 44.82 | 0.45 | 28.06 | 9.59 | 3.5 | 26 |
| 2 | 16.69 | 60.47 | 0.51 | 16.96 | 5.36 | 2 | 15 |
| 3 | 19.23 | 51.70 | 0.55 | 21.53 | 7.00 | 4 | 18 |
| 4 | 21.33 | 36.64 | 0.39 | 31.31 | 10.33 | 4 | 40 |
| 5 | 16.65 | 69.92 | 0.27 | 9.83 | 3.33 | 1 | 6 |
| 6 | 10.02 | 60.52 | 0.40 | 21.09 | 7.97 | 1.5 | 11 |
| 7 | 9.40 | 69.57 | 0.33 | 15.46 | 5.24 | 0.5 | 9 |
| 8 | 13.13 | 56.60 | 0.24 | 22.89 | 7.14 | 2 | 16 |
| 9 | 12.38 | 63.17 | 0.29 | 18.22 | 5.93 | 1.5 | 12 |
| 10 | 13.34 | 58.03 | 0.37 | 21.46 | 6.81 | 2 | 14 |

keep them in mechanical contact with the vertex of the quartz rod at constant pressure. Pressure was maintained at 200 g between the rod and the sample for the duration of the scan. AR scans were first collected with a white noise excitation source created in Matlab. A battery-powered MP3 player (Nike, Beaverton, OR) was used to supply the Matlab-generated noise signal, keeping 60 Hz noise to a minimum. The signal was passed through an operational amplifier before excitation of the PZT. The PZT detector output signal was collected using a 16-bit computer card (Realtek AC97, Realtek Semiconductor Japan, Yokohama, Kanagawa, Japan) for processing and analysis in Matlab 7.0.1 (The Mathworks Company, Natick, MA, USA). MANOVA was performed to identify the most significant frequencies, which were subsequently used for the construction of the ISP excitation source. ISP-ARS data were collected with the weight function calculated using MANOVA. The excitation signal consisted of three frequency ensembles in sequence, 1 s of each, for a total of 3 s of excitation. The incoming voltage signal was summed for each frequency mixture, and the integrated amplitude for each frequency became a single dimension in the classification procedure.

## Results and Discussion

Three excitations were employed for classification purposes. These three frequency ensembles were visualized as the three dimensions of an *XYZ* plot. As with all clustering algorithms, scans from similar samples tend to cluster together in hyperspace, while dissimilar samples tend to cluster in different regions of hyperspace. Therefore, projecting the three integrated signals from a sample scanned at the three frequency ensembles onto a three-dimensional plot quickly indicates to which class each sample belongs. Replicate scans of samples of the same type of fuel allow an analyst to, in effect, draw probability contour plots, localized around the regions of highest probability. This approach forms an electronic (analog) alternative to the digital calculation of probability densities for a given analyte.

*ARS vs ISP-ARS* Figure 3 illustrates the separation between clusters with conventional AR spectrometry. Principal components (PC) were calculated from the frequency range 14–17 kHz, and the three PCs that captured the largest variation were plotted against each other. It is apparent from the figure that there was very little difficulty distinguishing between groups of six samples of each different fuel mixture. Figure 4 illustrates the probability plots as calculated from the ISP-ARS data. In place of PC scores on the axes, the *XYZ* coordinates represent the detector voltages from each frequency ensemble selected by MANOVA integrated over time. All clusters from both methods contain six sample points, and the ellipses represent the 3 SD level in all directions about the centroid of the clusters.

Comparison of Figs. 3 and 4 indicate that there were notable differences between the ARS and ISP-ARS predictions. While both plots were drawn with 3 SD contours about their centroid, the clusters appear smaller with ISP-ARS. Fuel types 8 and 9 are exceptionally well differentiated from the others by ISP-ARS using the MANOVA-selected excitation. This result makes all of the clusters appear smaller in Fig. 4. If white noise is present and the noise power at each frequency is the same, the inclusion of more frequencies increases the total noise included in the PC model. On the other hand, the calculation of PCs across a wide frequency range tends to mask the effects of an erroneous measurement at one frequency. In the ISP-ARS model, however, one erroneous measurement can potentially have a larger effect on the actual projected point in hyperspace.

To illustrate the differences between ARS and ISP-ARS in a quantitative fashion, the bootstrap error-adjusted single sample technique (BEST), a nonparametric cluster algorithm, was used to calculate multidimensional standard deviations (MSD) between clusters [15]. Table 1 reports the MSDs calculated from the ARS, using the full spectral region spanning 14–17 KHz. Table 2 reports the MSDs calculated from the ISP-ARS clusters using a weighted subset of the same region. Distances in SDs greater than 3 are considered separable. ARS resulted in an average BEST MSD of 1164.24 between the clusters, while ISP-ARS resulted in an average BEST MSD of 109.44. The average cross-validation MSD was 1.41 for the ARS and 1.58 for the ISP-ARS. Both ARS and ISP-ARS were completely effective in classifying the fuel mixtures for the PillSafe, but only ISP-ARS could be implemented on a production line using an MP3 player without a computer.

*Versatility and Flexibility of ISP-ARS* ARS has previously been applied to the study of tablets [13–14], semisolids, and colloidal dispersions [15–16], liquids [17–19], and powders [20–22]. Clearly, ARS can be used for the analysis of samples in many phases. For any analyte that can be characterized or quantified by conventional ARS, an analogous ISP waveform can be programmed for the same analyte. However, the ISP process can be much simpler to use. For example, if a process requires a waveform to quantify the active pharmaceutical ingredient in a pharmaceutical tablet, experimenters could simply download the ISP waveform from an online

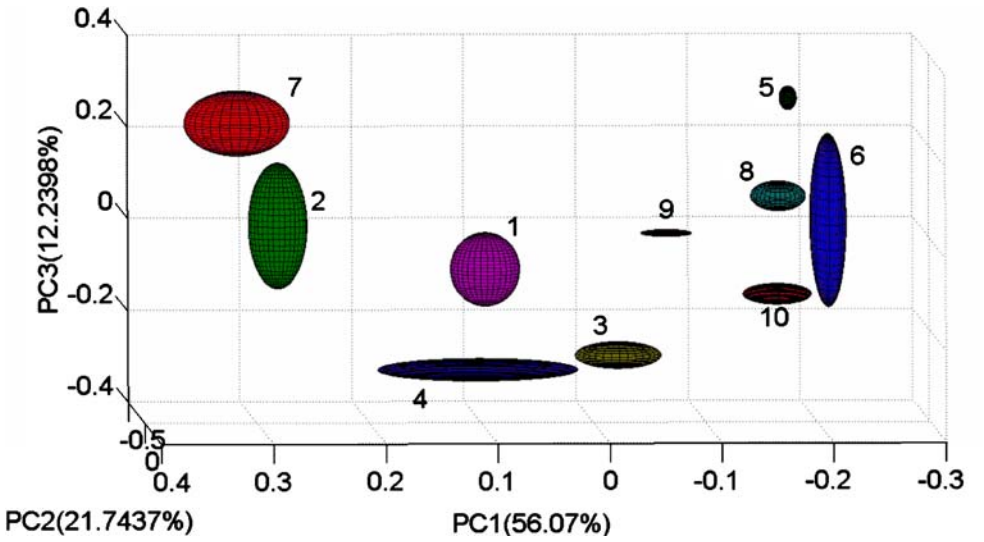


**Fig. 3** The three-principal components that capture the largest amount of variance can be projected into three-dimensional principal component space for easy visualization of the clusters. No a priori knowledge was included in the formation of this plot; therefore; the underlying data structure is clearly different for each fuel premix

database to an MP3 player. A database of ISP waveforms can easily be assembled to accommodate almost any experimental need. The ease of implementation makes ISP-ARS an attractive and potentially versatile method of analysis.

*Speed of Method* The data collection process itself is very rapid for both FT-ARS and ISP-ARS. No sample preparation is required, and all spectral data files for this research were collected for 3 s. The data analysis for FT-ARS, however, requires more time because it necessitates a digital post-processing step to yield useful information about a sample. Therefore, analysis times vary with the size of the data matrices for FT-ARS. On the other hand, ISP-ARS automatically outputs the analyte classification without the need for further computation. Therefore, for ISP-ARS, a total of only 3 s are necessary for simultaneous data collection and analysis.

*Figures of Merit* In multivariate data where the concentrations of multiple species are changing simultaneously, calculation of standard figures of merit (FOM), such as dynamic range, limit of detection, selectivity, sensitivity, and signal-to-noise ratio is not a straightforward task [23, 24]. The portion of the signal directly related to the analyte of interest is complicated by the signals from all other species and interferences present in the sample and sampling process. One good way to assess these quantities directly is by calculation of the net analyte signal (NAS), or the portion of the signal directly related to the analyte of interest, orthogonal to all interfering species. Once the NAS is known, the relationship between system constituents and the analytical signal can be quantified directly. However, calculation of the NAS requires pure component spectra from each of the analytes present in the system. For the purposes of this research, NAS is not a reasonable approach. For example, both the casting resin and the

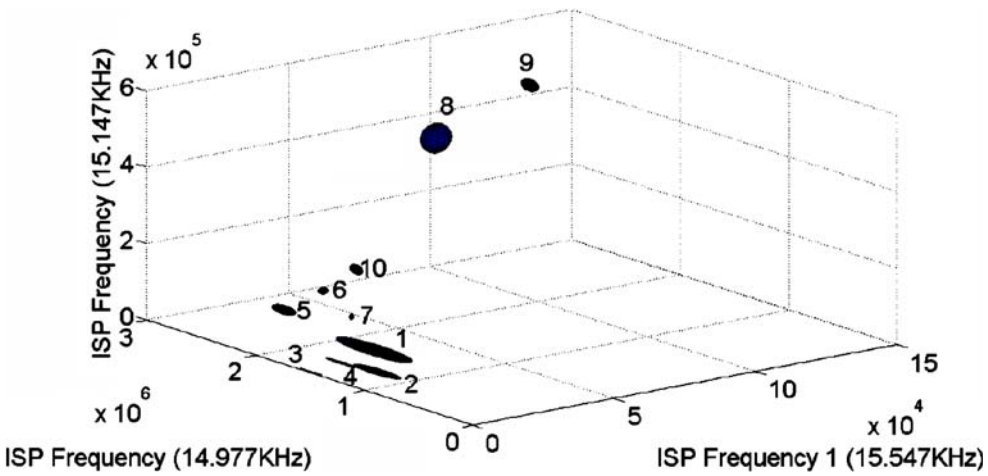


**Fig. 4** Full spectrum ARS spectra can be reduced to three-dimensional data with the MANOVA selection of the most distinguishing frequencies, followed by excitation and data collection using those three frequencies. Contour plots drawn in 3 SDs indicate the separation of each mixture from all the others. Each *ellipse* contains six points, taken from repeat scans of the same analyte

**Table 2** BEST distances calculated between mixture groups from 14 to 17 KHz

| Mixture number | 1 | 2 | 3 | 4 | 5 | 6 | 7 | 8 | 9 | 10 |
|---|---|---|---|---|---|---|---|---|---|---|
| 1 | 1.379 | 24.316 | 191.080 | 111.270 | 6429.500 | 28.959 | 224.420 | 713.400 | 12.847 | 80.220 |
| 2 | – | 1.469 | 146.720 | 289.110 | 9472.700 | 45.320 | 138.940 | 3433.400 | 94.000 | 112.530 |
| 3 | – | – | 1.326 | 172.790 | 186.340 | 150.290 | 185.140 | 185.170 | 205.290 | 200.360 |
| 4 | – | – | – | 1.578 | 507.430 | 18.634 | 92.031 | 51.252 | 321.790 | 57.694 |
| 5 | – | – | – | – | 1.310 | 980.150 | 783.200 | 11542.000 | 1367.200 | 530.100 |
| 6 | – | – | – | – | – | 1.398 | 76.344 | 145.720 | 100.520 | 32.220 |
| 7 | – | – | – | – | – | – | 1.433 | 7985.600 | 2045.000 | 51.177 |
| 8 | – | – | – | – | – | – | – | 1.456 | 1108.200 | 22.166 |
| 9 | – | – | – | – | – | – | – | – | 1.446 | 1738.200 |
| 10 | – | – | – | – | – | – | – | – | – | 1.288 |

Same-cluster BEST distances are reported on the diagonal. Every one of the mixtures was greater than 3 SDs from the others, indicating that the data were separable by the BEST metric.

curing agent are liquids before addition of the other. As soon as they are mixed, they react and solidify almost immediately. Clearly, the acoustic signals of the individual liquids do not combine in a linear fashion to form the acoustic signal of the combined solid.

Calculations of accuracy, precision, and bias are typically associated with calibration experiments, where the analytical signal varies with a change in concentration in some quantifiable fashion. This research however, was for classification purposes, so calculation of these values was again not as straightforward. The following is a description of the FOMs calculated and how each calculation was performed.

*Detection Limits* The detection limits were estimated by a mathematical translation of group populations $P_1$ and $P_2$ in hyperspace until they were no longer separable by the BEST metric [3]. For full spectrum ARS, the mean spectrum $(\overline{P})$ between 14 and 17 kHz is calculated for each population according to Eqs. 1 and 2.

$$\overline{P_1} = \frac{1}{m}\sum_{i=1}^{i=m} P_{1i} \tag{1}$$

$$\overline{P_2} = \frac{1}{m}\sum_{i=1}^{i=m} P_{2i} \tag{2}$$

A difference spectrum $X$ is calculated by $X = \overline{P_2} - \overline{P_1}$. The two populations are mathematically translated toward each other with $P_{\mathrm{ADJ}} = yX + \overline{P}_2$, where $y$ is a coefficient matrix defined on the interval $\{0<y<1\}$ until $P_{\mathbf{ADJ}}$ and $P_{\mathbf{1}}$ are inseparable by the BEST metric. To estimate the detection limits for each component, when the BEST MSD reaches three, the final value of $y$ is multiplied by the difference in component concentrations. Mixtures 1 and 2 were very close in BEST MSD for both full spectrum ARS and ISP-ARS, and they also had the most similar composition of all the mixtures; therefore, these samples were selected for the detection limit estimation calculation. The limit of detection for each mixture constituent was (reported as [ARS %, ISP-ARS %]): aluminum=[0.208, 0.176], $NH_4ClO_4$=[0.161, 0.136], $Fe_2O_3$=[0.004, 0.004], casting agent=[0.019, 0.016], and curing agent=[0.071, 0.060]. All values are reported in percent of the total mixture by mass. ARS populations could be translated 93.5% of the way toward each other in hyperspace before $P_1$ and $P_2$ were inseparable, and ISP-ARS populations were translated 94.5% of the way before $P_1$ and $P_2$ were inseparable. Therefore, ISP-ARS detection limits were slightly better than ARS for the measurement of each constituent in mixtures 1 and 2.

*Dynamic Range* The lower end of the dynamic range is set by the detection limit as described above. However, because the purpose of this research was not multivariate calibration, no upper-end limit could be explicitly calculated. Nevertheless, the largest concentration differences were between mixtures 4 and 8. Mixture differences are reported as the range (%) of mixture 7 relative to 8 (aluminum=[62.3%], $NH_4ClO_4$=[153.1%], $Fe_2O_3$=[39.8%], casting agent=[73.2%], and curing agent=[73.3%]). In calculation of the BEST MSDs for ISP-ARS, mixtures 7 and 8 had the largest separation. However, for full spectrum ARS, the MSD separation between these two mixtures was the second highest (please refer to Tables 2 and 3). These results suggest that in ARS, when mixtures are exceedingly different, MSD separation is not a linear indicator of the degree of separation, and as such, is not linearly related to changing concentrations. This conclusion is further supported by the ellipse plot in Fig. 3. While mixtures 7 and 8 are clearly very far apart, they are not the most distant clusters in the representation. These results indicate that for estimation of dynamic range, BEST MSDs are useful for

**Table 3** BEST distances calculated between mixture groups the ISP data

| Mixture number | 1 | 2 | 3 | 4 | 5 | 6 | 7 | 8 | 9 | 10 |
|---|---|---|---|---|---|---|---|---|---|---|
| 1 | 1.3077 | 9.5919 | 8.7532 | 7.0301 | 17.226 | 188.93 | 107.89 | 71.959 | 115.52 | 86.179 |
| 2 | – | 1.1945 | 20.746 | 9.7224 | 34.897 | 242.78 | 211.67 | 89.636 | 120.54 | 91.587 |
| 3 | – | – | 1.9609 | 10.488 | 49.573 | 190.47 | 124.72 | 59.833 | 123.84 | 70.847 |
| 4 | – | – | – | 1.9276 | 34.788 | 208.25 | 142.59 | 68.896 | 109.94 | 81.359 |
| 5 | – | – | – | – | 1.4752 | 34.403 | 15.312 | 43.868 | 260.47 | 21.665 |
| 6 | – | – | – | – | – | 1.8081 | 77.534 | 260.87 | 406.41 | 38.502 |
| 7 | – | – | – | – | – | – | 1.9659 | 327.08 | 314.64 | 154.45 |
| 8 | – | – | – | – | – | – | – | 1.6026 | 17.564 | 66.52 |
| 9 | – | – | – | – | – | – | – | – | 1.5495 | 175.07 |
| 10 | – | – | – | – | – | – | – | – | – | 0.96632 |

Same-cluster BEST distances are reported on the diagonal. Every one of the mixtures was greater than 3 SDs from the others, indicating that the data were separable by the BEST metric.

the low-end calculation. But for the high end of the dynamic range, BEST MSDs are not necessarily the most accurate representation of the actual chemical concentrations giving rise to differences between AR spectra. Conversely, in ISP-ARS, the BEST MSD between mixtures 7 and 8 is the largest degree of separation of all the mixtures, which agrees with the known constituent differences, suggesting that BEST MSDs calculated from ISP-ARS clusters continue to vary linearly with changing concentration. In future studies, the ISP-ARS will be used for sample quantification rather than identification; therefore, it will be a straightforward task to verify this observation.

*Signal-to-Noise, Precision, and Accuracy* The signal-to-noise ratio (*S*/*N*) was calculated as the mean amplitude of the signal divided by the SD of repeated measurements. The *S*/*N* ratios were [ARS=24.87, ISP-ARS=28.87]. Both *S*/*N* were of the same approximate magnitude. The precision is a measure of how repeatable each scan was for each mixture, expressed as the spread of repeated measurements relative to their total magnitude, or the inverse of the *S*/*N* ratio. The precisions were [ARS=0.040, ISP-ARS=0.035]; thus, the precision was slightly better for ISP-ARS. In qualification experiments, the accuracy can be measured by sensitivity TP/(TP FN) and specificity TN/(FP TN), where TP=the number of true positives, FP= the number of false positives, FN=the number of false negatives, and TN=the number of true negatives. As no samples were misidentified in cross-validation, the sensitivity and specificity were each 100%.

*Freedom from Interferences* The main sources of potential interference in both ARS and ISP-ARS are (1) radio frequency (RF) cross-talk between transmitting and receiving PZTs, (2) sound waves propagating through the support structures of the instrument, and (3) erroneous mechanical and electrical noise bursts. (1) RF cross-talk was addressed by suspending two PZT transducers in mid-air 10 cm apart from each other with no mechanical contact. Using one PZT in transmission mode and the other in collection mode, the noncontact mode signal strength was assessed. It was determined that the noncontact mode signal was negligible compared to the contact mode signal. In addition, in its operational configuration, both the transmitting and receiving PZTs are fastened with epoxy to the quartz rod; therefore, they do not move unless excited by mechanical contact. (2) The support structures for the ARS were made from wood, thus, inhibiting aberrant waveforms from propagating through the beams. Wood is made up of a cellular network of pores that convert sound energy into heat by frictional and viscoelastic resistance [26]. The cellular pore network creates high internal friction; therefore, wood has more sound-dampening capacity than most structural materials (e.g., steel, aluminum, or glass), thus, less sound traveled through the beams than if they had been made of metal. By coupling the quartz rod to the support structure through rubber grommets, an additional measure of dampening kept the sound interference to a minimum. Finally, the support structure was fixed in place and did not change during the course of the experiment, so interferences propagating through were the same for all sample and reference measurements. (3) All waveforms were programmed and generated synthetically in Matlab; therefore, they were tightly regulated for unwanted characteristics, such as spontaneous noise bursts, so the sound files for the broadband white noise source and the ISP waveform were clean. However, the excitation signal was passed through a dual-supply 741 operational amplifier to drive the transmitting PZT to full capacity. Electronic interference from electrical outlets, lights, computers, or radios all emit unwanted radiation that was picked up and amplified by the

amplifier. To address this issue, all electronic components associated with this research were battery powered. All scans were collected with the lights out and power sources unplugged from the outlets. In this manner, interferences were kept to a minimum.

## Conclusion

Integrated sensing and processing acoustic resonance spectrometry has demonstrated the ability to perform favorably with conventional acoustic resonance spectrometry. With a specifically tailored excitation signal selected from a library stored on an MP3 player, the ISP-ARS outputs the analyte identity directly and requires no post-collection analysis, thus, reducing data collection times and sparing the post-collection computational burden associated with ARS. An ISP waveform can easily be tailored for characterization or quantification of many types of analytes, enabling process simulations to be programmed to scan for analytes and process characteristics important to the simulation.

**Acknowledgement** This research was supported, in part, by NSF CNS-0540178, NIH N01AA33003, and the Kentucky Science and Engineering Foundation.

## References

1. Kunkler-Peck AJ, Turvey MT. Hearing shape. J Exp Psychol Hum Percept Perform 2000;26:279–94, (February).
2. Woodcock J. US Food and Drug Administration. http://www.fda.gov/ohrms/dockets/ac/02/briefing/3869B1_08_woodcock/sld001.htm. Retrieved Oct. 6, 2006.
3. Kac M. Can one hear the shape of a drum? Am Math Mon 1966;73(part II):1–23.
4. Gordon C, Webb D, Wolpert S. Isospectral plane domains and surfaces via Riemannian orbifolds. Invent Math 1992;110:1–22.
5. Chapman SJ. Drums that sound the sameAmer Math Monthly 1995;102:124–38.
6. Cipra B. You can't hear the shape of a drum. Science 1992;255:1642–3.
7. Buser P, Conway J, Doyle P, Semmler K. Some planar isospectral domains. Int Math Res Not 1994;391–400.
8. Berard P. Transplantation et isospectralite. Math Ann 1992;292:547–59.
9. Kuttler JR, Sigillito VG. Eigenvalues of the Laplacian in two dimensions. SIAM Rev 1984;26:163–93.
10. Bank R. PLTMG Users' Guide 7.0: A software package for solving elliptic partial differential equations. Philadelphia, PASIAM 1994.
11. Fox L, Henrici P, Moler C. Approximations and bounds for eigenvalues of elliptic operators. SIAM J Numer Anal 1967;4:89–102.
12. DARPA Defense Sciences Office. "Integrated sensing and processing." Retrieved 02 May 2006. http://www.darpa.mil/dso/thrust/math/isp.htm/.
13. Buice RG Jr, Pinkston P, Lodder RAA. pp Spec 1994;(4)84:517–24.
14. Medendorp JP, Lodder RA. Acoustic-resonance spectrometry as a process analytical technology for rapid and accurate tablet identificationAAPS PharmSciTech 2006;7(1):Article 25. DOI 10.1208/pt070125.
15. Medendorp JP, Buice RG Jr, Lodder RA. AAPS PharmSciTech 2007 (in press).
16. Dukhin AS, Goetz PJ. Langmuir. 1996;12:4987–97.
17. Kaatze U, Wehrmann B, Pottel RJ. Phys E: Sci Instrum 1987;20:1025–30.
18. Bolotnikov M, Neruchev Y. J Chem Eng Data 2003;48:411–5.
19. Leveque G, Ferrandis J, Van Est J, Cros B. Rev Sci Instrum 2000;71(3):1433–40.
20. Serris E, Camby-Perier L, Thomas G, Desfontaines M, Fantozzi G. Powd Tech 2002;128(2–3):296–9.
21. ReynaudP, Dubois J, Rouby D, Fantozzi G. Ceram Intern 1992:18 (6):391–7.
22. Martin L, Poret J, Danon A, Rosen M. Mat Sci Eng. 1998; A252:27–35.
23. Medendorp JP, Fackler JA, Henninger T, Dieter W, Lodder RAJ Pharm Innov 2006;1:54–61.
24. Medendorp JP, Lodder RA. J Chemometrics 2005;19:533–2.
25. Krzanowski, WJ. Principles of multivariate analysis. Oxford University Press, 1988.
26. Western Red Cedar Physical Properties. Bear Creek Lumber. Retrieved 1 March 2005 http://www.bearcreeklumber.com/generalinfo/onlineliterature/technicalinfohtml/wrcphysicalproperties.html/.